Nonlinear mechanisms for gain adaptation in locust photoreceptors

A. E. C. Pece,* A. S. French,* M. J. Korenberg,‡ and J. E. Kuster*
*Department of Physiology, University of Alberta, Edmonton, Alberta T6G 2H7; and ‡Department of Electrical Engineering, Queen's University, Kingston, Ontario K7L 3N6 Canada

ABSTRACT Intracellular membrane potential responses were recorded from locust photoreceptors under two stimulus conditions: pairs of flashes to dark-adapted receptors, and white-noise modulated light at a range of background intensities from 500 to 15,000 effective photons per second. Nonlinear analysis of the input–output relationships were performed by estimating the Volterra and Wiener kernels of the system. The Volterra kernels obtained from the double-flash experiments were similar to the Wiener kernels obtained from the white-noise experiments, except for a change of time scale. The structure of the second-order kernels obtained with either method gave evidence for a gain control mechanism acting at an early stage of the cascade. Both feedforward and feedback nonlinearities could account for the observed system behavior at any one background level. The differences in amplitude between the kernels obtained at different background levels could be accounted for by an adaptation process which further decreased the gain of the system, acting on a slower time scale, also at some early stage of the cascade.

INTRODUCTION

The responses of vertebrate photoreceptors to light have been shown to be mediated by a biochemical cascade between photon absorption by rhodopsin and the modulation of ion channels (for a review, see e.g., Lamb, 1986). There is reason to believe that the responses of invertebrate photoreceptors are mediated by similar mechanisms (Fein, 1986). Linear analysis of the response of *Limulus* photoreceptors to light provided evidence for such a cascade model of phototransduction before any chemical component of this system had been identified (Fuortes and Hodgkin, 1964).

When the light intensity is low enough to prevent saturation at any stage, a simple cascade of first-order reactions would result in a linear relationship between light stimulus and photoreceptor response, but some experimental observations, and particularly sublinear summation of elementary responses (reviewed by Laughlin, 1981, pp. 202–280), superlinear intensity dependence of the early phase of the response (Payne and Fein, 1986; Grzywacz et al., 1988), and adaptation, cannot be explained by a simple linear model of phototransduction. However, these observations are still compatible with cascade models of slightly greater sophistication.

Early studies of insect photoreceptors employing white-noise stimuli demonstrated a small second-order component of the response (Eckert and Bishop, 1975; Gemperlein and McCann, 1975). Recently, nonlinearities have been demonstrated when only a few (French and Kuster, 1985) or even single (Grzywacz and Hillman, 1985) photons have been transduced. In addition, the first-order Wiener kernel of the photoreceptor response has been shown to be affected by background light intensity (Kuster and French, 1985), an effect which can only be explained by nonlinear mechanisms.

In this paper we return to the analysis of insect photoreceptor responses to flashes and white noises. We show that the system kernels obtained by the two methods are similar and that some simple nonlinear models of gain control can account for their shape. These findings have some implications for the biophysical mechanisms involved because they support models in which the gain control lies at an early stage in the biochemical cascade of phototransduction.

The gain control process which we investigated occurs within the time scale of the transduction process; we believe that this process underlies the sublinear summation of responses found in photoreceptors of several different species (Laughlin, 1981), or at least contributes to the phenomenon. Other factors regulate the gain of phototransduction at time scales which are orders of magnitude slower (see for instance Claßen-Linke and Stieve, 1986). We will refer to these latter processes as adaptation and to the fast gain control process which we investigated simply as gain control for brevity. The relative amplitudes of the gain control and the transduction

Address correspondence to Dr. A. S. French.

0006-3495/90/04/733/11 $2.00

processes indicate that the inputs to both processes are scaled by the same factor as a function of background intensity. This would be expected if adaptation takes place at a stage within the phototransduction cascade located upstream from the stage where the gain control process branches off from the cascade because in this case the inputs to both processes would be scaled by the same factor.

METHODS

Preparation

Locusts, *Locusta migratoria*, were maintained in a laboratory colony under a 12-h light, 12-h dark photocycle. They were used 1–2 wk after their imaginal moult and dark adapted for at least 1 h before the experiment. The wings and legs were removed and the animal was immobilized with dental wax. Care was taken to avoid obstructing any of the respiratory spiracles. Experiments were performed at room temperature.

Stimulation

Light stimulation was provided by a green high-intensity light-emitting diode (HPHLMP 3950; Hewlett-Packard Co., Palo Alto, CA) held by a Cardan arm at a distance of 5 cm from the eye. The stimulus was generated by a 33-bit shift register clocked at 1 kHz (Marmarelis and Marmarelis, 1978) to give a pseudo-random binary sequence, which was then filtered by a nine-pole active low-pass filter (corner frequency: 50 Hz) and a single-pole high-pass filter (corner frequency: 0.05 Hz). A DC component was then added to the signal. The DC level and power level of the signal were adjusted independently. The signal was used to drive the light-emitting diode (LED) via a constant current circuit. For each DC level, the power level was set as high as possible while maintaining the LED forward polarized.

Recordings

Glass microelectrodes filled with 3 M potassium acetate and having a resistance of 50–100 MΩ were lowered through a hole in the cornea of the right eye to penetrate retinular cells. The reference silver chloride electrode was placed in the left eye. Intracellular voltage was measured by a conventional amplifier (model 5; Getting Inc., Los Altos, CA), high pass filtered at 0.05 Hz by a single-pole filter and low-pass filtered at 100 Hz by a single-pole filter. The LED current and the intracellular voltage were sampled at 10-ms intervals and stored on-line in a digital computer. The photoreceptor response contains very little signal above a frequency of 50 Hz (the Nyquist frequency for a sampling interval of 10 ms). Low-pass filtering was used only to limit the random noise of the recordings.

Conversion from LED current to LED light intensity was done off-line for each sample point by a program using a calibration curve obtained by means of a phototransistor (MRD 3050; Motorola Inc., Schaumberg, IL). Instantaneous light intensities could be converted to effective photons per second (ep/s, i.e., photons effectively transduced) by counting the frequency of bumps (single photon responses) at a low steady level of illumination (producing 5–10 ep/s) and then extrapolating to higher light intensities. This calibration was only approximate because it was often difficult to distinguish single photon responses from random noise in the voltage trace on the oscilloscope. Of course, any error in the calibration would affect all background level measurements by the same factor, leaving the relative levels unchanged.

The methods used for the double-flash experiments were very similar and have been described previously by French and Kuster (1985). The sampling interval for the double-flash experiments was 5 ms, but in this analysis pairs of adjacent voltage samples were averaged together to produce records with an effective sampling interval of 10 ms, equal to the interval used in the white-noise experiments.

THEORY

Feedforward gain control

We analyzed four different models which can account for the nonlinearities which we observed experimentally. Each of these four models includes two distinct processes, a linear transduction process K and a linear gain control process G, and these two processes interact nonlinearly. The four models differ in structure (feedforward or feedback) and in the nature of the nonlinear interaction between the processes, as explained in detail below.

A simple feedforward gain control scheme is shown in Fig. 1 *a*. The rectangular boxes are dynamic linear filters with delta responses $g(u)$ and $k(v)$, whereas the static nonlinear element N performs the operation:

$$z(t) = x(t)\{1 - s(t)\}, \tag{1}$$

where t is time, $x(t)$ is the input signal, and the other signals are as labeled in Fig. 1 *a*. Eq. 1 may be expanded as follows:

$$z(t) = x(t) - \int g(u)x(t)x(t-u)\,du \tag{2}$$

and therefore:

$$y(t) = \int k(v)x(t-v)\,dv - \iint k(v)g(u)x(t-v)x(t-u-v)\,du\,dv. \tag{3}$$

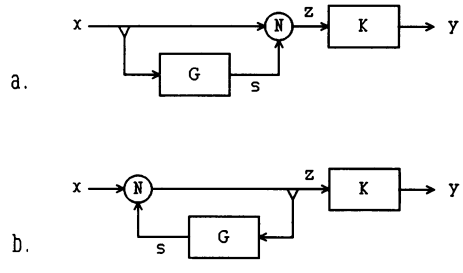

FIGURE 1 Minimum separable models of gain control. (*a*) feedforward model; (*b*) feedback model. The elements G and K are dynamic linear, whereas the element N is static nonlinear. The operation performed by this latter element can be a multiplication as in Eq. 1 or a division as in Eq. 9. The upturned triangles highlight the branching point of the gain control process from the transduction process.

Substituting $w = u + v$, and assuming that $g(u) = 0$ for $u < 0$:

$$y(t) = \int k(v)x(t - v)\,dv - \iint k(v)g(w - v)x(t - v)\,x(t - w)\,dw\,dv. \quad (4)$$

Approximating the system by a Volterra series, or functional expansion:

$$y(t) = h_0 + \int h_1(a)x(t - a)\,da + \iint h_2(a, b)x(t - a)x(t - b)\,da\,db + \ldots \quad (5)$$

Then by comparison of Eqs. 4 and 5 the Volterra kernels of the system are given by: $h_0 = 0$, $h_1(a) = k(a)$, $h_2(a, b) = -1/2[g(a - b)k(b) + g(b - a)k(a)]$, and all higher-order kernels are identically zero. Here we have followed the convention that the second-order kernel is symmetric in its arguments. Indeed, with this convention the second-order kernel can be reduced to $h_2(a, b) = -(1/2)g(w - v)k(v)$, where $w = \max(a, b)$ and $v = \min(a, b)$ because $g(t) = 0$ if $t < 0$. However, for simplicity we shall use triangular second-order kernels, i.e., kernels which are identically zero unless $0 \leq b \leq a$, so that $h_2(a, b) = -g(a - b)k(b)$.

Feedback gain control

A simple feedback gain control system is shown in Fig. 1 *b*, with similar linear and nonlinear elements to those of Fig. 1 *a*. The nonlinear element again performs the operation given by Eq. 1 so that its output, $z(t)$, may be expressed as follows:

$$z(t) = x(t) - \int g(u)x(t)z(t - u)\,du. \quad (6)$$

Eq. 6 is a Fredholm integral equation of the second kind (Davis, 1962) and cannot be solved analytically. A series approximation to Eq. 6 may be developed by expanding the term in $z(t)$ within the convolution integral, introducing new time variables where necessary, and assuming that the functions $g(u)$ and $k(v)$ are zero at negative times:

$$z(t) = x(t) - \int g(u)x(t)x(t - u)\{1 - \int g(w)z(t - u - w)\,dw\}\,du. \quad (7)$$

The output of the system, $y(t)$, may then be obtained from convolution of $z(t)$ with the final linear element, $k(v)$:

$$y(t) = \int k(v)x(t - v)\,dv - \iint k(v)g(u)x(t - v)x(t - u - v)\,du\,dv + \ldots \quad (8)$$

If the system output is again approximated by a Volterra series, as in Eq. 5, then the Volterra kernels in triangular format become: $h_0 = 0$, $h_1(a) = k(a)$, $h_2(a, b) = -g(a - b)k(b)$, $h_3(a, b, c) = g(a - b)g(b - c)k(c)$, etc. These kernels are identically zero unless $0 \leq c \leq b \leq a$.

Gain control by a ratio nonlinearity

If the equation describing the nonlinear elements N in Fig. 1 is:

$$z(t) = x(t)/\{1 + s(t)\} \quad (9)$$

instead of Eq. 1, we have a system which is more difficult to describe by Volterra kernels, but which might be biologically more realistic, as we will discuss in Conclusions. With Eq. 9 as the nonlinear operation, the output of the system in Fig. 1 *a* becomes:

$$y(t) = \int k(v)x(t - v)/\{1 + \int g(u)x(t - v - u)\,du\}\,dv, \quad (10)$$

whereas the output of the system in Fig. 1 *b* becomes:

$$y(t) = \int k(v)x(t - v)/\{1 + \int g(u)z(t - v - u)\,du\}\,dv. \quad (11)$$

By expanding the fraction in Eq. 9 into a MacLaurin series, it can be shown that the first and second terms of the series are identical to the right-hand side of Eq. 1. Therefore, the first- and second-order Volterra kernels will be identical for systems containing the product (Eq. 1) or ratio (Eq. 9) nonlinearities. This can also be shown by expanding Eqs. 10 and 11 into MacLaurin series: in this case, the first- and second-order terms of the series become identical to those in Eqs. 3 and 8. However, the four systems produce different outputs because they differ in their higher-order kernels.

Separability in the second-order kernel

Eqs. 3 and 8 both predict that the second-order Volterra kernel, $h_2(a, b)$ should be separable into two functions, $g(u)$ and $k(v)$, if it is first rearranged to give a new second-order kernel:

$$p_2(u, v) = h_2(u + v, v) \quad (12)$$

so that:

$$p_2(u, v) = -g(u)k(v). \quad (13)$$

However, Eq. 3 predicts that a complete description of the system output can be obtained from $h_1(u)$ and $h_2(u, v)$, whereas Eq. 8 indicates that even a simple feedback nonlinear system requires an infinite series to represent the system behavior. Both equations also predict that the first-order kernel, $h_1(u)$, should be identical to the delta

response of the linear system which is in series with the nonlinearity.

The variables u and v in the above equations can be interpreted as the difference $\Delta\tau$ between the two time variables and the smaller time variable τ of the second-order kernel $h_2(\tau + \Delta\tau, \tau)$. This notation is particularly useful for understanding the experimental meaning of the second-order kernel obtained in the double-flash experiments, in which u (i.e., $\Delta\tau$) is the interflash interval and v (i.e., τ) is the time after the second flash.

From our analysis in the previous section it follows that Eqs. 12 and 13 are still valid if the nonlinearity is of the form of Eq. 9. However, in this case even a feedforward system requires an infinite series of Volterra kernels. We will refer to the models of Fig. 1 as separable models, irrespective of the kind of nonlinearity, and, if the second-order kernel is said to be separable, it is understood that it is separable after a coordinate transformation according to Eq. 12.

Computational methods

Volterra kernels were computed from single- and double-flash responses by the method first introduced by Schetzen (1965). The method can be briefly described as follows: If we assume that all higher-order nonlinearities are negligible at the stimulus intensities that were used, the response to a single flash will be

$$y_1(\tau) = h_1(\tau) + h_2(\tau, \tau), \tag{14}$$

where τ is the time after the flash, h_1 the first-order Volterra kernel, and h_2 the second-order Volterra kernel. The response to a double flash will be:

$$\begin{aligned} y_2(\tau, \Delta\tau) = {} & h_1(\tau) + h_2(\tau, \tau) + h_1(\tau - \Delta\tau) \\ & + h_2(\tau - \Delta\tau, \tau - \Delta\tau) \\ & + 2h_2(\tau, \tau - \Delta\tau) = y_1(\tau) \\ & + y_1(\tau - \Delta\tau) + 2h_2(\tau, \tau - \Delta\tau), \end{aligned} \tag{15}$$

where $\Delta\tau$ is the time interval between the first and the second flash, and τ is again the time after the first flash. $h_2(u, v)$ was calculated from $y_1(\tau)$ and $y_2(\tau, \Delta\tau)$, using Eq. 15. Then, $h_1(u)$ was calculated from $y_1(\tau)$ and $h_2(\tau, \tau)$ (i.e., the diagonal of h_2) using Eq. 14. To calculate $h_2(u, v)$ over a square region with equal spacing between samples along both the u and v axes, one alternative is to record responses to pairs of flashes with interflash intervals varying between 0 and 250 ms in steps of 10 ms. However, we used responses obtained with interflash intervals between 0 and 150 ms, varying in steps of 25 ms. With intervals of > 150 ms, there were no significant second-order responses. The missing intervals below 150 ms were obtained by cubic spline interpolation.

Wiener kernels were computed from white-noise experiments using the fast orthogonal algorithm. This method was described previously by Korenberg (1988), and one of its first applications to a biological system by Korenberg et al. (1988). For our experiments, we found that reliable second-order kernels could only be extracted from records of at least 40,000 data pairs. Records of even greater length were required if extraneous noise (especially photon noise at low background levels) was present.

The second-order kernels obtained by both methods are the symmetrical $h_2(a, b)$ as shown in Fig. 2; we converted these to triangular format by eliminating all values above the diagonal and doubling all values below the diagonal. The kernels $p_2(u, v)$ could then be obtained by a simple coordinate transformation. Each kernel p_2 was stored in computer memory as a square matrix; to extract the delta response $g(u)$ (which is a one-dimensional array) the three rows which correspond to the highest values of $h_1(v)$ were averaged, i.e, if the time to peak of $h_1(v)$ was v_p, we averaged $p_2(u, v_p - 1)$, $p_2(u, v_p)$, and $p_2(u, v_p + 1)$ to obtain $-g(u)$. Once g was calculated, the three columns of p_2 corresponding to the highest values of g were averaged to obtain an estimate of k which we call k_p and which we expect to be identical to h_1.

Simulations of any of the various models were done by explicitly computing the values of all the signals in the corresponding diagram of Fig. 1 at 10-ms intervals. The outputs of the linear components were obtained by convolution and the output of the static nonlinear component by simple algebra. The estimate of k which we used in our simulations was h_1 because the first-order component of the photoreceptor output is larger than the second-order component and therefore its estimate is likely to be more accurate. Unless otherwise specified, for our simulations k and g were scaled by finding scaling factors for each of them which would minimize the mean-square error between the experimental output and the simulated output over a record segment of 3,000 data pairs. The scaling factors were found by an iterative procedure. Similar scaling factors were obtained for all models if the input to the simulated models was only the AC white-noise component of the experimental stimulus. The kernels shown in Figs. 5 and 6 were scaled under these conditions.

RESULTS AND DISCUSSION

Flash experiments

The results of the flash experiments have been published and discussed previously (French and Kuster, 1985). Here we return to them to extract Volterra kernels from the impulse responses.

The response of a system to even a single impulse contains all the nonlinearities of any order present in the

system. However, for small stimuli, it is often possible to ignore nonlinearities above a certain order. In this case, we are interested in extracting first- and second-order Volterra kernels from single- and double-flash responses. In these experiments, the flash intensity was adjusted so that each flash resulted in about one photon being transduced on average. A total of 93 flash responses for each delay between flashes were averaged. The second-order kernel shown in Fig. 2 contains the short-lasting facilitation (thinner contour lines in the lower left corner) and the longer-lasting depression (thicker contour lines) already discussed by French and Kuster (1985). A later positive deflection is also evident in the upper right corner; this second-order depolarization might represent no more than a sublinear increase of the hyperpolarization observed in the first-order kernel. The first-order kernel h_1 is shown in Fig. 3 and is not very different from the system impulse response.

The question is whether the second-order kernel is separable. To answer this, the transformed kernel $p_2(u, v)$ was obtained by a change of coordinates and then the delta responses $g(u)$ and $k_p(v)$ were extracted as described in the previous section. The results are shown in Fig. 3. $k_p(v)$ appears to be very similar to $h_1(v)$. Note that $g(u)$ seems to reach a maximum for an interflash interval u of ~30 ms, but the resolution along the u axis is limited by the fact that, in this experiment, interflash intervals varied in steps of 25 ms, as explained in the previous section. Experiments with better resolution demonstrate that the maximum second-order effect is

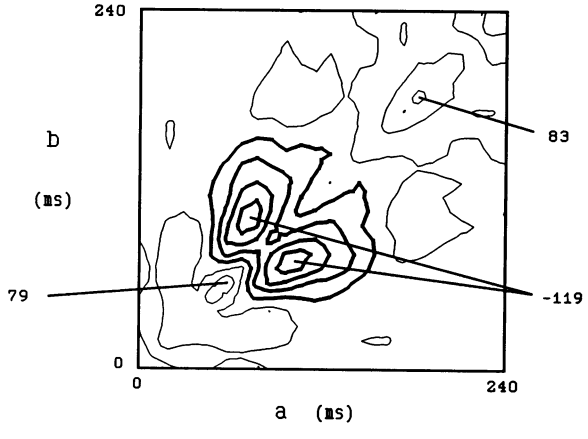

FIGURE 2 The second-order Volterra kernel $h_2(a, b)$ obtained from flash experiments following the approximative method described under Eqs. 14 and 15. This kernel is shown in symmetrical format, so that the kernel values are half as large as the values in Fig. 4, which is obtained by coordinate transformation from a triangular kernel. Kernel values at the highest or lowest contours are given in $\mu V/ep^2$. Thicker (thinner) contour lines include areas of negative (positive) kernel values; all contour lines, irrespective of thickness, are separated from each other by 30 $\mu V/ep^2$.

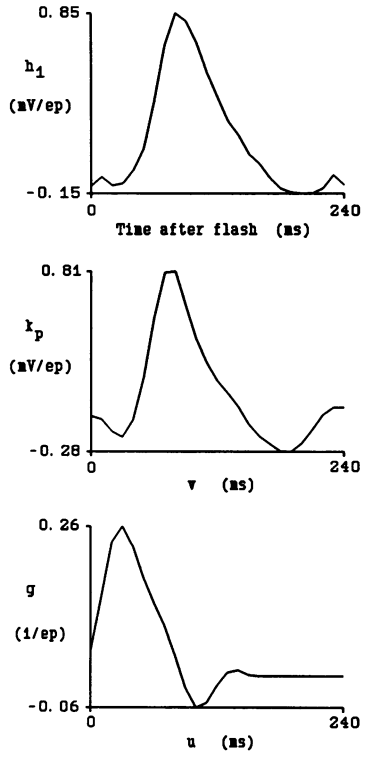

FIGURE 3 First-order Volterra kernel h_1 obtained from flash experiments and delta responses k_p and g of the dynamic linear elements K and G extracted from the corresponding second-order kernel. Units of h_1 and k_p are given in mV/ep, whereas units of g are given in ep^{-1}.

obtained with an interflash interval between 5 and 10 ms (Fig. 5 in French and Kuster, 1985). In Figs. 3 and 4, u corresponds to the time interval between flashes and v corresponds to the time after the second flash.

A further check for separability is the synthesis of $p_2(u, v)$ from the kernels $g(u)$ and $k_p(v)$. Fig. 4 shows the experimental and synthesized p_2 kernels. The main difference between the two kernels was the peak of facilitation at ~60 ms on the v axis of the experimental kernel (which corresponds to the diagonal of h_2).

We concluded that the double-flash responses contain at least one significant feature which cannot be explained by a separable model. Separable models can account for the decrease of gain in the response to the second flash, i.e., the depression described by French and Kuster (1985), but the faster time course of the response to the second flash, i.e., the early facilitation described by French and Kuster, cannot be explained by a separable model because the time course of the facilitation is not identical to the time course of the linear response, $h_1(t)$.

White-noise experiments

First- and second-order Wiener kernels were measured at a range of background intensities from 500 to 15,000

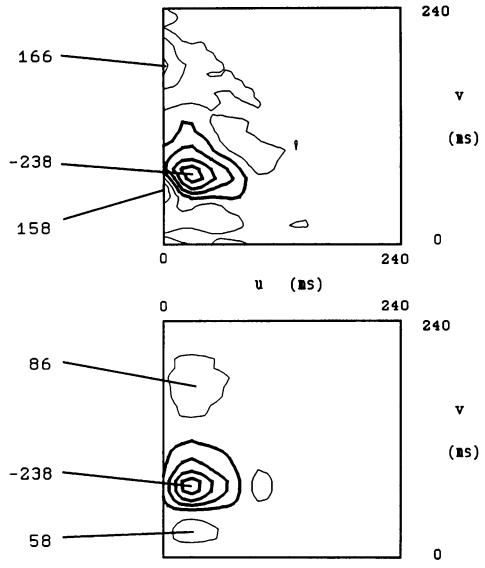

FIGURE 4 Upper: Second-order kernel p_2 obtained from the Volterra kernel of Fig. 2 by coordinate transformation as defined by Eq. 12. Lower: Synthesized kernel $p_2(u, v)$ obtained by multiplication of the linear kernels $k_p(v)$ and $v(u)$ shown in Fig. 3. Units on both contour maps are given in $\mu V/ep^2$. For both kernels, v is the time after the second flash and u is the interflash interval. Contour lines are separated from each other by 60 $\mu V/ep^2$.

ep/s. The noise power level of the input signal was always made as high as possible without clipping the LED output, so the ratio of mean background amplitude to noise power level was always approximately the same. As shown in Fig. 5, the first-order kernel became faster when the background was increased from 500 to 2,300 ep/s, but further increases only affected the gain and not the time course of the first-order kernel. The noise of the recordings, and especially the photon noise, limited considerably the accuracy of the second-order kernels measured at < 500 ep/s, but the first-order kernel appeared to become even slower at lower background levels.

All the kernels in Fig. 5 were obtained from the same cell. It can be seen that the $k_p(v)$ kernel extracted from $p_2(u, v)$ was very similar to the first-order Wiener kernel at every background level. Both $k_p(v)$ and $g(u)$ changed in amplitude with changing background and changed in time course only at the lowest background levels, in the same manner as the first-order kernel.

Fig. 6 shows the experimental kernel $p_2(u, v)$ and the synthesized $p_2(u, v)$ from $k_p(v)$ and $g(u)$ for the same background levels as in Fig. 5. The main features of the experimental kernels are a small facilitation low on the v axis (clearly resolved only at 500 ep/s), a slightly delayed inhibition just off the v axis, and a later (upper) facilitation, with the inhibition being much stronger than either facilitatory component, as in the double-flash experiments. When the background level was increased, the

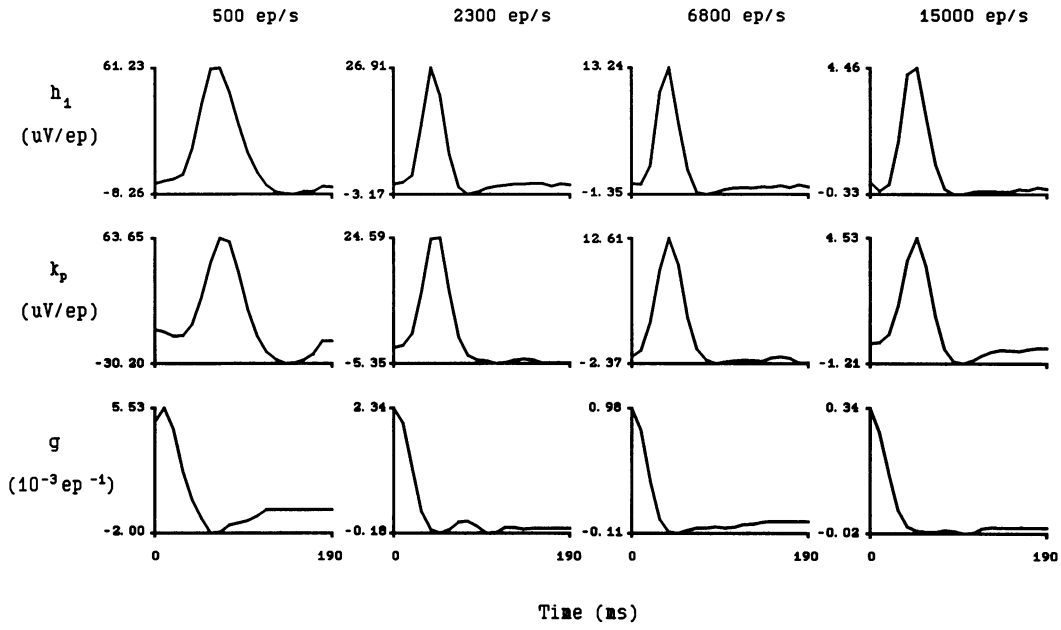

FIGURE 5 Linear kernels obtained from white-noise experiments at the background levels indicated along the top of the figure. Kernels are shown normalized to the same size for purposes of comparison. Absolute amplitudes were affected by the stability of the recordings, but the relative sizes of h_1, k_p, and g were fairly constant, except at the lowest background level.

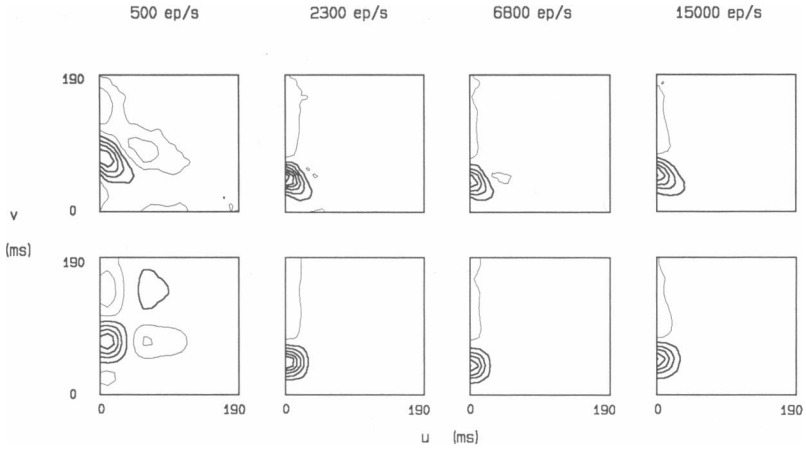

FIGURE 6 Second-order kernels p_2 obtained with white-noise stimulation at the background levels indicated along the top of the figure. Upper: from h_2 by coordinate transformation. Lower: synthesized from k_p and g. Contour lines are separated by 80 nV/ep^2 (500 ep/s), 10 nV/ep^2 (2,300 ep/s), 2nV/ep^2 (6,800 ep/s), 0.3 nV/ep^2 (15,000 ep/s).

early facilitation became negligible. At all background levels, especially above 500 ep/s, the experimental $p_2(u, v)$ kernel could be synthesized fairly accurately from g and k_p. A partial overlap between early facilitation and inhibition could account for the skewness of the inhibitory component observed at both background levels as well as in the double-flash experiment. This interpretation would agree with our conclusion that only the early facilitation cannot be accounted for by a separable model.

Simulations

To test the predictive power of the different models described in Theory, we tried to reproduce the responses of photoreceptors by computer programs that simulated such models. At low power levels, the first- and second-order Wiener kernels of any system can be approximated by their Volterra equivalents (the relationship between Volterra and Wiener kernels is given by Marmarelis and Marmarelis, 1978, p 150). This approximation depends on the assumption that higher-order nonlinearities are negligible. Under this assumption, we carried out two kinds of simulations. First, we tried to reproduce the photoreceptor output by simulating a first-order Volterra system with the first-order kernel h_1 or a second-order Volterra system with the kernels h_1 and h_2. In the second kind of simulation, the kernels h_1 and g of Fig. 5 were used as the delta responses of the linear components K and G of the models of Fig. 1; the models were simulated with both kinds of nonlinear element (product, Eq. 1 and ratio, Eq. 9). The Volterra simulations and the model simulations are compared with the actual experimental output in Fig. 7.

The mean-square error between the linear simulation and the experimental response was ~17% of the output power of the experimental response, i.e., the first-order kernel accounted for ~83% of the response. The exact values of these percentages varied in different sections of the records. Linear simulations are, of course, unaffected (except for a DC offset) by any background superimposed on the white noise. Second-order Volterra simulations as well as simulations of any of the models could be done using either the actual input (background plus white noise) or its AC component (white noise only). In the kernel computations, we used only the AC components of the input, subtracting the background level. The resulting Wiener kernels approximate Volterra kernels for negative or positive stimuli superimposed on this background level. For this reason, the simulations too were performed using the AC component of the input only. The mean-square error of the model simulations were ~16% of the output power, i.e., the nonlinear component of the model responses accounted for an additional 1% of the response. The penultimate trace shows the response of the second-order Volterra system. The error of this simulation was ~15% of the output power. The significance of a nonlinear mechanism which apparently contributes so little to the photoreceptor response will be discussed in Conclusions.

We tried simulating responses obtained at a high background level using kernels obtained at a lower background level. In this case, the DC component of the input was not completely subtracted, but adjusted relative to the level at which the kernels were obtained (e.g., if the kernels were obtained at a background level of 2,300 ep/s, this latter value was subtracted from the real input being used in the experiment, leaving a smaller but considerable

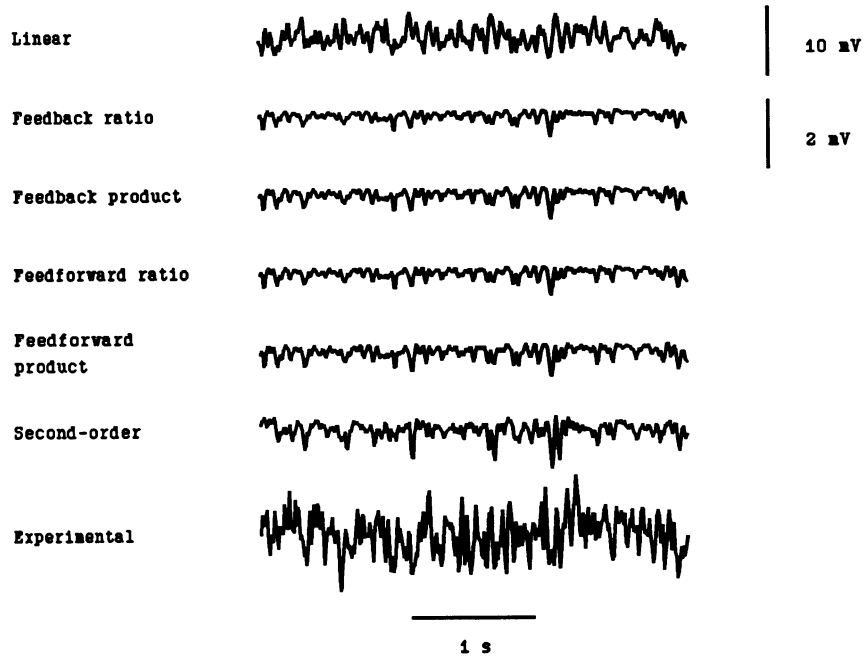

FIGURE 7 First trace: simulated linear component of the photoreceptor potential response to white-noise stimulation at a background level of 6,800 ep/s. The other traces represent differences from this trace, at a different scale, of the simulations of the output produced using separable models (traces 2–5) or a Volterra second-order model (trace 6), or of the experimental trace (lowest trace), as indicated. The kernels used for the simulations were obtained from a larger record including the segment shown here. For these simulations, the background was subtracted from the input signal (not shown). The mean-square error of the linear model simulation was ~17% of the output power; the mean-square errors of the separable model simulations were ~16%; the mean-square error of the second-order model simulation was ~15%.

DC component). Most of these simulations produced responses which were either larger in amplitude than the experimental responses, or very different in shape, or even inverted in polarity. This discrepancy is likely to be due to an adaptation phenomenon at some point in the phototransduction pathway which decreases the signal amplitude in proportion to the background level. This adaptation process could be located either before or after the G branch separates from the K branch at the site indicated by a triangle in Fig. 1. It is clear that in the first case, the gain of both branches would be equally affected by the background level, whereas in the second case only the gain of the K branch would be affected. The first hypothesis is favored by the fact that the ratios of the h_1 and g kernel amplitudes are similar at all background levels.

CONCLUSIONS

We have tried to demonstrate that separable models of the transduction and gain control processes can describe the results of two very different experimental protocols with considerable accuracy. Support for this conclusion comes from the similarities between the two estimates of k (from h_1 and from h_2, as described in Theory) obtained at any background light level, as well as from the agreement between simulated and experimental responses.

Location of the gain control points at the first stages of the cascade would be functionally useful because any stage located before the gain control point could be saturated by a high input level. Similarly, location of a slower adaptation site before the branch-point of the gain control process prevents its saturation, except during transients. In our experimental conditions, separable models offer little improvement of the fit over the linear model. However, fast gain control might be most relevant to photoreceptor function when there is a sudden shift in background level, e.g., when the animal flies from the shade into sunlight. In these conditions, a fast process of gain control might be very important until slower adaptation processes take place. This suggests that comparisons between simulated model responses and instantaneous intensity-response functions (Laughlin, 1981) could provide clearer evidence for or against the various separable models. In this respect, it may be pointed out that the power level of a symmetric binary stimulus is much higher than that of pseudo-random white noise (Larken et al., 1979), for equal background levels. The double-flash

stimulus is an asymmetric binary stimulus, in which the background level is kept low by using a very short duty cycle and therefore the power level is even higher than for a symmetric binary stimulus with the same background level. Because the nonlinear components of the response are relatively larger at higher power levels (the linear component is proportional to the power level, whereas the second-order component is proportional to the square of the power level), the double-flash experiments should produce relatively much larger nonlinear components of the response, as indeed was the case.

It should be pointed out that the Wiener kernels obtained by Larken et al. (1979) from human electroretinographic (ERG) responses are similar in some respects to those we obtained because the ERG kernels also seem to be separable, except for an initial facilitation. Furthermore, the response time courses become faster with increased background levels both in the human ERG and in the locust receptor potential. We were motivated to investigate separable models primarily by S. Klein's analyses of the ERG responses (manuscript in preparation). An important question is whether separable models only describe the input–output relationship of the system or whether they contain important features of the underlying biophysical mechanisms.

We have pointed out three major discrepancies between the predictions of the separable models and the experimental results. One of these, the early facilitation, is most evident in the double-flash experiments: Any separable model is bound to predict only a change of amplitude, and not of time course, in the flash responses. This early facilitation is also present, but less evident, in the p_2 kernels obtained from the noise experiments. The other two discrepancies are the changes in the amplitude and time course of the linear kernels k and g as the background level is increased (the time course being affected only below 2,300 ep/s).

The dependence of kernel amplitude on background level is greater than can be accounted for by the models themselves. This is demonstrated by the fact that accurate simulations of the responses obtained at higher background levels cannot be obtained with kernels at low background levels. This finding requires that we introduce a slower (adaptation) process in our models. This additional parameter is of course justified by the extensive evidence for adaptation processes in the time scales of seconds to minutes.

Both the facilitation observed in the p_2 kernels and the dependence of the photoresponse time course on background level are also well-known phenomena (Payne and Fein, 1986; Grzywacz et al., 1988; Laughlin, 1981). Whether they are due to the same mechanism remains to be established.

The discrepancies that we observed do not demonstrate that separable models are inadequate biophysical models of the fast gain control process but simply indicate that there are other processes going on at the same time during phototransduction. These processes cannot be definitively identified by system analysis and modeling techniques alone. It is possible that they are not independent from each other. One model which could account for the observed fast gain control process and could incorporate the additional processes for which we have evidence is shown in Fig. 8. In this model, the input signal is processed by three linear stages, whereas a feedback signal originates between stages G and J and controls the gain in the nonlinear element N. We suggest that in locust photoreceptors the first stage F is static linear, i.e., it acts simply as a scaling factor on the input, whereas stages G and J are dynamic linear. Slow adaptation processes regulate the gain of stages F and/or G, whereas the time constants of stages G and/or J could be regulated by both fast and slow processes. Neglecting all these additional factors, the system is equivalent to the one represented in Fig. 1 *b*, with K = GJ and F being simply a multiplicative constant.

Other models, e.g., feedforward models, are compatible with our results, but we believe that there are some reasons to favor a feedback mechanism. In a feedforward model it would not be possible to incorporate the linear stage G into the phototransduction cascade, and a model in which the gain control transmitter is the same as one of the chemical components of the cascade (a mechanism known as "product inhibition") seems simpler than one in which the gain control branch requires a separate biochemical mechanism, as the schemes in Fig. 1 seem to imply. In addition, the error of the simulated response of the feedback ratio model is the least sensitive to changes in the amplitude of the g kernel. Perhaps most important, however, is that the fractional power-law relationship between intensity and response (Laughlin, 1981, Eq. E.2), which is found with flash stimuli in photoreceptors of several species, is identical, except for a different notation and the inclusion of a saturation effect, to an equation derived from a feedback model of enzyme

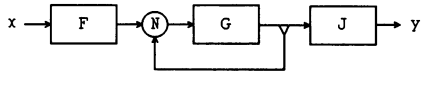

FIGURE 8 A hypothetical mechanism of phototransduction and gain control compatible with the results presented here. The elements F, G and J are cascades of first-order reactions. The reactions lumped into F are not rate limiting because they are faster than the reactions lumped into the other stages (i.e., F is a static linear element). The element N is static nonlinear and is described by Eq. 9. The physical mechanism of this nonlinearity could be enzyme inhibition. The upturned triangle highlights the branching point of the gain control process.

inhibition by Grzywacz and Hillman (1988, Eq. 8). This latter equation was derived for adaptation to steady light, not for fast gain control in flash responses, but the two phenomena are apparently similar except for a difference in time scale.

The biochemical equivalent of the separable model is a cascade with a control point for the gain placed before any of the rate-limiting steps. If this nonlinear gain control is accomplished by inhibition of an enzyme, Eq. 9 might be a reasonable mathematical approximation of the nonlinear element (Grzywacz and Hillman, 1988). This equation arises from the assumption that the gain at stage N is proportional to the fraction of enzyme which is not bound to its inhibitor. We point out that although a feedback mechanism is generally less stable than a feedforward mechanism, a ratio nonlinearity increases the stability of the system as compared with a multiplicative nonlinearity.

Gain control at stage N implies some gain at this stage. According to our hypothesis, this stage would be located before any rate-limiting step in the transduction process. In *Limulus* photoreceptors the average delay of single photon responses ("bumps") is twice their average duration, which has been shown to be incompatible with any cascade model in which there is gain at or before the first rate-limiting step (Schnakenberg and Keiper, 1986). However, the ratio between these two parameters is quite different for bumps from locust photoreceptors, for which the average delay is about equal to the average half-duration (Howard, 1983; Pece and French, 1989). The phototransduction process is much faster in insects than it is in *Limulus,* so that even if the biochemical components are the same, the detailed kinetic parameters are certainly quite different. Therefore, it seems likely that at least some of the kinetic differences between phototransduction mechanisms in *Limulus* and locust are located in stage F. According to our hypothesis, in locust photoreceptors the time constants of this stage are negligible compared with the time constants of the following stages. Statistics of bump parameters also indicate that nonlinear processes are much less important in *Limulus* than in locust photoreceptors at low light levels (Grzywacz and Hillman, 1985).

The evidence from research on adaptation favors a feedback mechanism as well. Fuortes and Hodgkin (1964) already found some evidence in favor of a feedback mechanism in *Limulus* photoreceptors. More recently, Grzywacz and Hillman (1988) have shown that only a negative feedback mechanism can account for the observed sublinear relationship between steady-state light intensity and steady-state depolarization of *Limulus* ventral photoreceptors. The current biochemical model of phototransduction in vertebrates also includes a feedback pathway for adaptation (for a short review, see Pugh and Altman, 1988). Functional similarities in the transduction and adaptation mechanisms of different animal groups might be obscured by differences in the kinetics or in the polarity of the photoresponses.

We were introduced to separable models by Dr. S. A. Klein (University of California, Berkeley) at the workshop on Advanced Methods of Physiological System Modeling chaired by Dr. V. Z. Marmarelis of the Biomedical Simulations Resource at the University of Southern California. We thank Dr. Klein for helpful discussion

Support for this work was provided by the Medical Research Council of Canada, the Alberta Heritage Foundation for Medical Research, the Natural Sciences and Engineering Research Council of Canada, and the Advisory Research Committee of Queen's University.

Received for publication 7 July 1989 and in final form 6 December 1989.

REFERENCES

Claßen-Linke, I., and H. Stieve. 1986. The sensitivity of the ventral nerve photoreceptor of *Limulus* recovers after light adaptation in two phases of dark adaptation. *Z. Naturforsch. Sect. C Biosci.* 41c:657–667.

Davis, H. T. 1962. Introduction to nonlinear differential and integral equations. Dover Publications, New York. 566 pp.

Eckert, H., and L. G. Bishop. 1975. Nonlinear dynamic transfer characteristics of cells in the peripheral visual pathway of flies. Part I: The retinula cells. *Biol. Cybern.* 17:1–6.

Fein, A. 1986. Excitation and adaptation of *Limulus* photoreceptors by light and inositol 1,4,5-trisphosphate. *Trends Neurosci.* 9:110–114.

French, A. S., and J. E. Kuster. 1985. Nonlinearities in locust photoreceptors during transduction of small numbers of photons. *J. Comp. Physiol. A Sens. Neural Behav. Physiol.* 156:645–652.

Fuortes, M. G. F., and A. L. Hodgkin. 1964. Changes in time scale and sensitivity in the ommatidia of *Limulus*. *J Physiol.* (*Lond.*). 172:239–263.

Gemperlein, R., and G. D. McCann. 1975. A study of the response properties of retinula cells of flies using nonlinear identification theory. *Biol. Cybern.* 19:147–158.

Grzywacz, N. M., and P. Hillman. 1985. Statistical test of linearity of photoreceptor transduction process: *Limulus* passes, others fail. *Proc. Natl. Acad. Sci. USA.* 82:232–235.

Grzywacz, N. M., and P. Hillman. 1988. Biophysical evidence that light adaptation in *Limulus* photoreceptors is due to a negative feedback. *Biophys. J.* 53:337–348.

Grzywacz, N. M., P. Hillman, and B. W. Knight. 1988. The quantal source of area supralinearity of flash responses in *Limulus* photoreceptors. *J. Gen. Physiol.* 91:659–684.

Howard, J. 1983. Variations in the voltage response to single quanta of light in the photoreceptors of *Locusta migratoria. Biophys. Struct Mech.* 9:341–348.

Korenberg, M. J. 1988. Identifying nonlinear difference equation and functional expansion representations: the fast orthogonal algorithm. *Ann. Biomed. Eng.* 16:123–142.

Korenberg, M. J., A. S. French, and S. K. L. Voo. 1988. White-noise analysis of nonlinear behavior in an insect sensory neuron: kernel and cascade approaches. *Biol. Cybern.* 58:313–320.

Kuster, J. E., and A. S. French. 1985. Changes in the dynamic properties of locust photoreceptors at three levels of light adaptation. *Biol. Cybern.* 52:333–337.

Lamb, T. D. 1986. Transduction in vertebrate photoreceptors: the roles of cyclic GMP and calcium. *Trends Neurosci.* 9:224–228.

Larkin, R. M., S. Klein, T. E. Ogden, and D. H. Fender. 1979. Nonlinear kernels of the human ERG. *Biol. Cybern.* 35:145–160.

Laughlin, S. B. 1981. Neural principles in the visual system. *In* Handbook of Sensory Physiology VII/6B. Autrum, editor. Springer-Verlag, Berlin. 133–280.

Marmarelis, P. Z., and V. Z. Marmarelis. 1978. Analysis of physiological systems. The white-noise approach. Plenum Press, New York. 487 pp.

Payne R., and A. Fein. 1986. The initial response of *Limulus* ventral photoreceptors to bright flashes. Released calcium as a synergist to excitation. *J. Gen. Physiol.* 87:243–269.

Pece, A. E. C., and A. S. French. 1989. Single photon responses in locust photoreceptors: the effects of stimulus location on amplitude and time course. *J. Comp. Physiol. A Sens. Neural Behav. Physiol.* 164:365–375.

Pugh, E., and J. Altman. 1988. A role for calcium in adaptation. *Nature* (*Lond.*). 334:16–17.

Schetzen, M. 1965. Measurement of the kernels of a nonlinear system of finite order. *Int. J. Contr.* 1:251–263.

Schnakenberg, J., and W. Keiper. 1986. Experimental results and physical ideas towards a model for quantum bumps in photoreceptors. *In* The molecular mechanism of photoreception. H. Stieve, editor. Springer-Verlag, Berlin. 353–367.